

# SU( $N$ ) Toric Code and Nonabelian Anyons

Manu Mathur <sup>1</sup>, Atul Rathor <sup>2</sup>

S. N. Bose National Centre for Basic Sciences  
JD Block, Sector III, Salt Lake City, Kolkata 700106, India

## Abstract

We construct SU( $N$ ) toric code model describing the dynamics of SU( $N$ ) electric and magnetic fluxes on a two dimensional torus. We show that the model has  $N^2$  topologically distinct ground states  $|\psi_0\rangle_{(\mathbf{p},\mathbf{q})}$  which are loop states characterized by  $Z_N \otimes Z_N$  centre charges ( $\mathbf{p}, \mathbf{q} = 0, 1, 2, \dots, N - 1$ ). We explicitly construct them in terms of coherent superpositions of all possible spin network states on torus with Wigner coefficients as their amplitudes. All excited quasiparticle states with SU( $N$ ) electric charges and magnetic fluxes are constructed. We show that the braiding statistics of these SU( $N$ ) electric, magnetic quasiparticles or nonabelian anyons is encoded in the Wigner rotation matrices.

## 1 Introduction

In the last few years topological quantum computing (TQC) with abelian, nonabelian anyons has become one of the most promising approaches for storing and processing quantum information reliably in systems on two dimensional surfaces [1, 2, 3]. In these computational approaches, the quantum information is encoded in the topological braiding of anyons, therefore making it resilient against any local perturbations or decoherence effects. All these models with anyons originated from the simple  $Z_2$  toric code model proposed by Alexei Kitaev in 1997 [1]. This (2 + 1) dimensional model is an exactly solvable model with 4 degenerate ground states which are characterized by  $Z_2 \otimes Z_2$  topological order. The anyonic excitations in this model and the topological nature of their braiding have led to the idea of topological or fault-tolerant quantum computers having an intrinsic resistance to small perturbations. In this work we generalize Kitaev's  $Z_2$  toric code model to SU( $N$ ) group leading to nonabelian anyons. In the recent past nonabelian anyons have been subject of intense research for their quantum computing applications [2, 3]. The SU( $N$ ) toric code model provides a natural setting for studying such nonabelian exotic quasiparticles. We show that the SU( $N$ ) toric code model has  $N^2$  degenerate ground states which are loop or spin network states and are characterized by  $Z_N \otimes Z_N$  topological charges. They are explicitly constructed in terms of spin networks and the Wigner coefficients. In fact, beside their topological stability, the ground states of SU( $N$ ) toric code model are also geometrically rigid because of the numerous inter-linked triangular electric flux constraints satisfied by the underlying spin network states<sup>3</sup> over the entire torus. This geometrical stability is purely a group theoretical property of the Hilbert space of the SU( $N$ ) toric code model. We also construct all excited states using SU( $N$ ) link holonomies and

---

<sup>1</sup>manu@boson.bose.res.in, manumathur14@gmail.com

<sup>2</sup>atulrathor@bose.res.in, atulrathor999@gmail.com

<sup>3</sup>In SU(2) case, there are  $2L^2$  triangular constraints on a torus with  $L^2$  lattice sites. The  $L = 2$  case with 8 triangular constraints on the torus is worked out completely (see section 2.1 and Figure 3).

nonabelian vortex creation-annihilation operator. We show that the  $SU(N)$  canonical commutation relations between electric fields and the conjugate potentials lead to nonabelian anyons. We further show that their mutual statistics is encoded in Wigner D matrices.

The plan of the paper is as follows. In section 2 we construct the  $SU(N)$  toric code model and the associated operators and their algebras are discussed. We assume basic familiarity with Hamiltonian formulation of lattice gauge theory. All the details of this Hamiltonian formulation, reviewed briefly in this section, are extensively discussed in the excellent original review article [4]. In section 2.1 we construct the ground state in the topologically trivial sector. In section 2.1.1 we extend this construction to include  $Z_N \otimes Z_N$  topological charges where  $Z_N$  is the center of the group  $SU(N)$ . The section 2.2 discusses the excited states of the  $SU(N)$  toric code Hamiltonian. In section 2.2.1 we discuss excitations with nonabelian electric charges. In section 2.2.2 we discuss the nonabelian magnetic excitations and the corresponding vortex operators [6]. In the last section we discuss the nonabelian anyonic nature of the above excitations.

Throughout this paper, we use the following notations: The lattice sites on the 2 dimensional torus, denoted by  $\mathcal{T}_2$ , are labeled as  $\vec{n} = (x, y); x, y = 1, 2, \dots, L$ . The lattice links are denoted by  $\vec{l} \equiv (\vec{n}; \hat{i})$  with  $i = 1, 2$ . We will often denote the sites by  $v$  or  $s$ , links by  $l$  and plaquettes by  $p$  for shorter notations if other details are not required. On the torus  $\mathcal{T}_2$  there are  $L^2$  sites,  $2L^2$  links and  $L^2$  plaquettes and the periodicities imply  $(x + L, y) = (x, y + L) = (x, y)$ . We will use  $SU(2)$  toric code to illustrate all explicit calculations. This makes the presentation simple. The higher  $SU(N)$  groups can also be similarly handled.

## 2 $SU(N)$ toric code model

We generalize Kitaev's  $Z_2$  toric code model to  $SU(N)$  group by considering the  $SU(N)$  link flux operators  $U_{\alpha\beta}(\vec{l})$  and the corresponding  $SU(N)$  electric fields  $E_{\pm}^a(\vec{l})$  ( $E_{\pm}^a(\vec{l})$ ) with  $\alpha, \beta = 1, 2, \dots, N$  and  $a = 1, 2, \dots, (N^2 - 1)$  [4]. These electric fields, shown in the Figure 1-a, rotate the link holonomies  $U(\vec{l})$  from the left (right) end respectively<sup>4</sup>. Therefore, we get the following canonical commutation relations

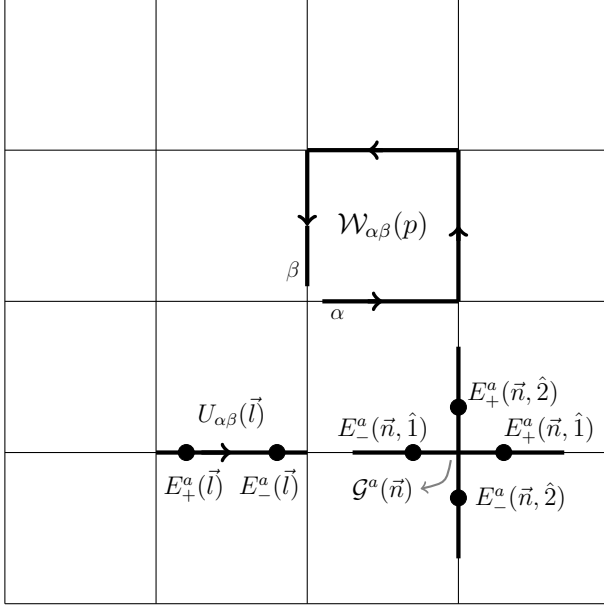
$$[E_{+}^a(\vec{l}), U_{\alpha\beta}(\vec{l})] = (T^a U(\vec{l}))_{\alpha\beta}, \quad [E_{-}^a(\vec{l}), U_{\alpha\beta}(\vec{l})] = -(U(\vec{l}) T^a)_{\alpha\beta}. \quad (1)$$

In (1)  $T^a$  are the generators in the fundamental representation of  $SU(N)$  satisfying  $\text{Tr}(T^a T^b) = \frac{1}{2}\delta_{ab}$ . The above commutation relations along with Jacobi identity yields [4]

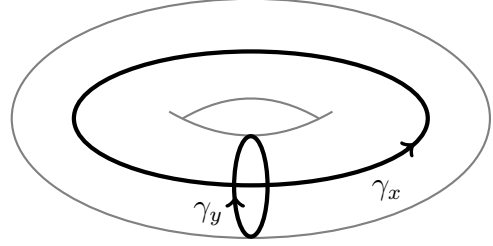
$$[E_{+}^a(\vec{l}), E_{+}^b(\vec{l})] = i f^{abc} E_{+}^c(\vec{l}), \quad [E_{-}^a(\vec{l}), E_{-}^b(\vec{l})] = -i f^{abc} E_{-}^c(\vec{l}). \quad (2)$$

---

<sup>4</sup>As shown in Figure 1-a:  $U(\vec{l}) \equiv U(\vec{n}, \hat{i})$ ,  $E_{+}^a(\vec{l}) \equiv E_{+}^a(\vec{n}; \hat{i})$  and  $E_{-}^a(\vec{l}) \equiv E_{+}^a(\vec{n} + \hat{i}; \hat{i})$



(a) SU(N) link fluxes & electric fields



(b) Flux loops  $\gamma_x$  and  $\gamma_y$  on  $\mathcal{T}_2$

Figure 1: (a) The conjugate SU(N) electric fields  $E_{\pm}^a(\vec{l})$  and link operators  $U_{\alpha\beta}(\vec{l})$ . The operators  $\mathcal{G}^a(\vec{n})$  and  $\mathcal{W}(p)$  appearing in the Hamiltonian (9) are also shown, (b) Two non-contractible Wilson loops  $\gamma_x$  and  $\gamma_y$  on the torus  $\mathcal{T}_2$ .

In (2)  $f^{abc}$  are the SU(N) structure constants. The left and the right electric fields in (1) are related by a parallel transport [4]:

$$E_-(\vec{l}) = -U^\dagger(\vec{l}) E_+(\vec{l}) U(\vec{l}). \quad (3)$$

In (3) we have defined  $E_{\pm}(l) \equiv \sum_a E_{\pm}^a(l) T^a$ . It is easy to check that on any link  $l = (\vec{n}; \hat{i})$ , the magnitude of the left and right electric fields are equal and they commute with each other

$$\text{Tr} \left( \vec{E}_+(\vec{l}) \cdot \vec{E}_+(\vec{l}) \right) = \text{Tr} \left( \vec{E}_-(\vec{l}) \cdot \vec{E}_-(\vec{l}) \right) \equiv \text{Tr} \vec{E}^2(\vec{l}), \quad (4a)$$

$$\left[ \vec{E}^2(\vec{l}), E_+(\vec{l}) \right] = 0, \quad \left[ \vec{E}^2(\vec{l}), E_-(\vec{l}) \right] = 0, \quad (4b)$$

$$\left[ E_+(\vec{l}), E_-(\vec{l}) \right] = 0. \quad (4c)$$

The important identities (4a), (4b) and (4c) imply that the Hilbert space in the simplest  $SU(2)$  case is spanned by the eigenvectors  $|j(l), m_+(l), m_-(l)\rangle \equiv |j, m_+, m_-\rangle_l = |j, m_+\rangle_l \otimes |j, m_-\rangle_l$  on every link  $l$  satisfying

$$\begin{aligned} (\vec{E}_{\pm}(l))^2 |j, m_+, m_-\rangle_l &= j(l)(j(l)+1) |j, m_+, m_-\rangle_l, \\ E_{\pm}^{a=3}(l) |j, m_+, m_-\rangle_l &= m_{\pm}(l) |j, m_+, m_-\rangle_l. \end{aligned} \quad (5)$$

The  $SU(N)$  transformations<sup>5</sup> on the flux operators  $U(\vec{n}; \hat{i})$  and electric fields  $E_{\pm}(n; \hat{i})$  are [4]

$$\begin{aligned} U(\vec{n}; \hat{i}) &\rightarrow \Lambda(\vec{n}) U(\vec{n}; \hat{i}) \Lambda^{\dagger}(\vec{n} + \hat{i}), \\ E_{\pm}(\vec{n}; \hat{i}) &\rightarrow \Lambda(\vec{n}) E_{\pm}(\vec{n}; \hat{i}) \Lambda^{\dagger}(\vec{n}) \quad i = 1, 2. \end{aligned} \quad (6)$$

In (6)  $\Lambda(\vec{n})$  are the  $SU(N)$  matrices describing  $(N^2 - 1)$   $SU(N)$  rotational degrees of freedom at every lattice site  $\vec{n}$ . The canonical commutation relations (1) imply that the generators of the above  $SU(N)$  rotations at site  $\vec{n}$  are

$$\mathcal{G}^a(\vec{n}) \equiv \sum_{i=1}^2 \left( E_+^a(\vec{n}; \hat{i}) + E_-^a(\vec{n}; \hat{i}) \right). \quad (7)$$

We also define  $SU(N)$  plaquette operators which contain  $SU(N)$  magnetic fields<sup>6</sup>

$$\mathcal{W}_{\alpha\beta}(p) = \left( U(\vec{n}; \hat{i}) U(\vec{n} + \hat{i}; \hat{j}) U^{\dagger}(\vec{n} + \hat{j}; \hat{i}) U^{\dagger}(\vec{n}; \hat{j}) \right)_{\alpha\beta}. \quad (8)$$

We now generalize Kitaev's toric code and write  $SU(N)$  toric code Hamiltonian as

$$H = A \sum_n A_n + B \sum_p B_p. \quad (9)$$

In the above Hamiltonian  $n$  and  $p$  denote the sites and plaquettes on the torus  $\mathcal{T}_2$ ,  $A$  and  $B$  are positive constants and

$$A_n \equiv \sum_{a=1}^{N^2-1} \mathcal{G}^a(n) \mathcal{G}^a(n), \quad B_p \equiv \text{Tr} (2N - \mathcal{W}(p) - \mathcal{W}^{\dagger}(p)). \quad (10)$$

Under  $SU(N)$  transformations (6) both electric and magnetic field terms in (7) and (8) respectively transform covariantly

$$\mathcal{G}(n) \rightarrow \Lambda(n) \mathcal{G}(n) \Lambda^{\dagger}(n), \quad \mathcal{W}(p) \rightarrow \Lambda(n) \mathcal{W}(p) \Lambda^{\dagger}(n). \quad (11)$$

In (11),  $\mathcal{G} \equiv \sum_a \mathcal{G}^a T^a$ . Therefore, toric code Hamiltonian in (9) is invariant under the  $SU(N)$  rotations (6). Like Kitaev's model, the Hamiltonian (9) is a sum of  $L^2$  electric terms,  $L^2$

---

<sup>5</sup>The transformations (6) are the  $SU(N)$  symmetries of the toric code Hamiltonian (9). They do not correspond to the redundancies in  $SU(N)$  gauge theory which are removed by the Gauss law constraints  $\mathcal{G}^a(n) = 0$  at every lattice site.

<sup>6</sup>The  $SU(N)$  magnetic fields on plaquette  $p$  are defined as  $B^a(p) \equiv \frac{1}{2} \text{Tr} T^a (2N - \mathcal{W}(p) - \mathcal{W}^{\dagger}(p))$ .

magnetic terms and they all commute with each other<sup>7</sup>

$$[A_n, A_{n'}] = 0, \quad [A_n, B_{p'}] = 0, \quad [B_p, B_{p'}] = 0. \quad \forall n, n', p, p'. \quad (12)$$

On a torus we have additional topological invariants defined over non contractible loops. These  $SU(N)$  Wilson loop operators in the fundamental representation are

$$W_{\gamma_x} = \text{Tr} \prod_{\vec{l} \in \gamma_x} U(\vec{l}), \quad W_{\gamma_y} = \text{Tr} \prod_{\vec{l} \in \gamma_y} U(\vec{l}) \quad (13)$$

In (13)  $\gamma_x$  and  $\gamma_y$  are the two independent oriented paths shown in Figure 1-b and the products over links are path ordered. The paths  $\gamma_x(\gamma_y)$  start from an arbitrary base point  $(x_0, y_0)$  and return to it after looping the torus in the horizontal (vertical) direction. It is easy to check that they satisfy

$$[W_{\gamma_x}, W_{\gamma_y}] = 0, \quad [W_{\gamma_x}, A_n] = 0, \quad [W_{\gamma_x}, B_p] = 0, \quad [W_{\gamma_y}, A_n] = 0, \quad [W_{\gamma_y}, B_p] = 0. \quad (14)$$

In the next section we will exploit (12) and (14) to characterize the topological sectors of  $SU(N)$  toric code model and construct the  $N^2$  ground states with topological charges.

## 2.1 Ground states

We first study the ground state structure of the  $SU(N)$  toric code Hamiltonian (9). A ground state  $|\psi_0\rangle$  satisfies

$$A_n |\psi_0\rangle = 0, \quad B_p |\psi_0\rangle = 0, \quad \forall n, p \in \mathcal{T}_2. \quad (15)$$

The first condition in (15) enforces  $SU(N)$  rotational invariance on the ground state  $|\psi_0\rangle$ . These constraints are same as  $(N^2 - 1)$   $SU(N)$  Gauss law constraints in  $SU(N)$  gauge theory. Therefore, all possible ground states of the  $SU(N)$  toric code Hamiltonian are the all mutually independent loop states of the  $SU(N)$  lattice gauge theory. These loop states are best analyzed and characterized in the dual electric flux basis [5]. We note that in two space dimensions there are 4  $SU(N)$  electric fluxes meeting at a vertex. Their quantum numbers can be characterized by the corresponding 4  $SU(N)$  Young tableaux. The Gauss law constraints  $A_v = 0$  states that the ground state manifold consists of all possible independent  $SU(N)$  invariant states with total  $SU(N)$  electric flux = 0. In the simple  $N = 2$  case [5] a basis in the loop Hilbert space at a vertex  $s$  is given by  $|j_1, j_2, j_{12} = j_{34}, j_3, j_4\rangle_s \equiv |\vec{J}\rangle_s$ . This is shown in Figure 2-c. They satisfy

$$\mathcal{G}^a(s) |\vec{J}\rangle_s = 0, \quad \forall s \in \mathcal{T}_2. \quad (16)$$

---

<sup>7</sup>The first two relations in (12) are the symmetry statements of the toric code Hamiltonian (9). The first equation follows from the fact that  $[\mathcal{G}^a(n), \mathcal{G}^a(n')] = 0 \forall n, n'$  because of the identity (4c). The second relation is because  $B_p$  is invariant under  $SU(N)$  rotations (6). The third relation is trivially true because all flux operators  $U_{\alpha\beta}(l)$  commute amongst themselves.

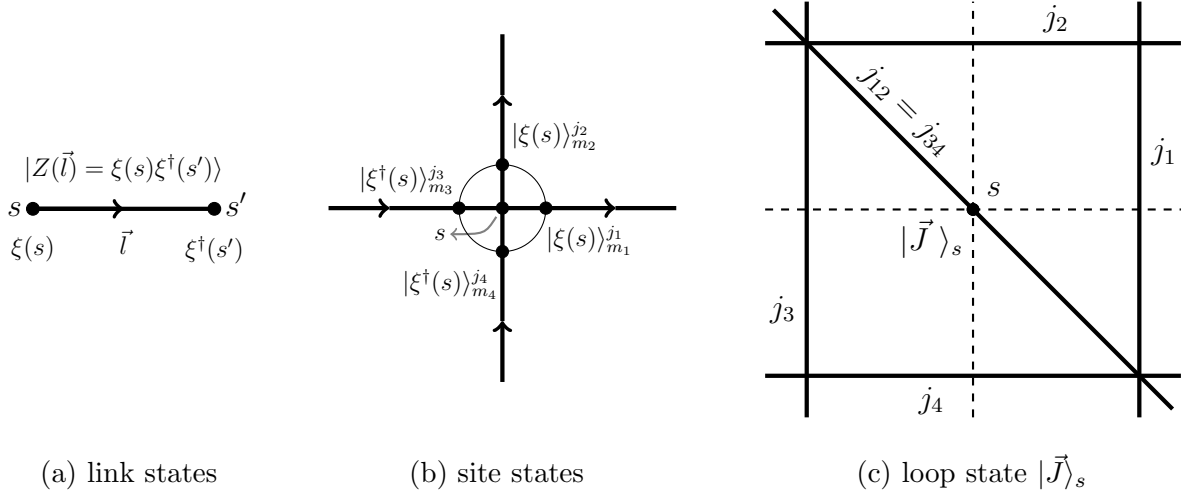


Figure 2: Ground states of toric code. From (a) link states  $|Z(\vec{l})\rangle$  to (b) site states  $|\xi(s)\rangle_m^j$  to (c) loop states  $|\vec{J}\rangle_s \equiv |j_1, j_2, j_{12} = j_{34}, j_3, j_4\rangle_s$ . The geometrical triangular constraints are manifest on the dual lattice (solid lines) around the site  $s$  in (c). Every lattice site has 2 triangular constraints.

Therefore, if we label the  $L^2$  vertices or sites on the torus by  $v_1, v_2, \dots, v_{L^2}$  then the ground state of SU(2) toric code is of the form:

$$|\psi_0\rangle = \sum_{\{\vec{J}_{v_1}, \vec{J}_{v_2}, \dots\}} \underbrace{W(\vec{J}_{v_1}, \vec{J}_{v_2}, \dots)}_{\text{amplitude on torus}} \underbrace{\left\{ \prod_{i=1}^{L^2} \otimes |\vec{J}\rangle_{v_i} \right\}}_{\text{loop states on torus}} \quad (17)$$

In (17) the summation over  $\{\vec{J}_{v_i}\}$  are constrained as each electric flux  $j(l)$  is shared by two vertices at the 2 ends of the link  $l$ . The first ground state condition  $A_v|\psi_0\rangle = 0$  is ensured by the spin network identities (16) for arbitrary amplitudes  $W(\vec{J}_{v_1}, \vec{J}_{v_2}, \dots)$ . These amplitudes are now fixed by demanding  $B_p|\psi_0\rangle = 0$ . However, we find this approach difficult as the action of  $B_p$  on a spin network state is not simple [5]. We therefore reverse the process and start with completely ordered magnetic eigenstates with  $B_p = 0, \forall p$  and then ensure  $A_v|\psi_0\rangle = 0$  by demanding invariance under the symmetry transformations (6) at every vertex. We first notice that the eigenstates of  $B_b$  in (10) are necessarily eigenstates of the individual link holonomies  $U(\vec{l})_{\alpha\beta}$ . As all these flux operators commute with each other  $[U_{\alpha\beta}(\vec{l}), U_{\gamma\delta}(\vec{l}')] = 0, \forall \vec{l}, \vec{l}'$  and  $\forall \alpha, \beta$ , we can diagonalize all of them simultaneously. For this purpose we first define SU(2) group manifold  $S^3$  on every link ( $l$ ):

$$Z(\vec{l}) = \begin{bmatrix} z_1(\vec{l}) & z_2(\vec{l}) \\ -z_2^*(\vec{l}) & z_1^*(\vec{l}) \end{bmatrix}. \quad (18)$$

In (18)  $(z_1, z_2) \in S^3$  and satisfy  $|z_1(\vec{l})|^2 + |z_2(\vec{l})|^2 = 1, \forall \vec{l}$ . We define the magnetic eigenstates to be eigenstates of each link operator:

$$U_{\alpha\beta}(\vec{l}) |Z(\vec{l})\rangle = Z_{\alpha\beta}(\vec{l}) |Z(\vec{l})\rangle. \quad (19)$$

The eigenvectors are

$$|Z(\vec{l})\rangle \equiv |z_1(\vec{l}), z_2(\vec{l})\rangle = \frac{1}{4\pi} \sum_{j=0}^{\infty} \sqrt{(2j+1)} \sum_{m_{\pm}} D_{m_+, m_-}^j(Z(\vec{l})) |j m_+\rangle_l \otimes |j m_-\rangle_l. \quad (20)$$

To obtain ground state with  $B_p = 0$  or equivalently  $\mathcal{W}_{\alpha\beta}(p) = \delta_{\alpha\beta}$  we choose pure gauge conditions on every link to write

$$Z(\vec{l}) \equiv Z(\vec{n}, \hat{i}) = \xi(s) \xi^\dagger(s') \quad (21)$$

as shown in Figure 2-a. At each site  $s \in \mathcal{T}_2$ ,  $(\xi(s) \equiv \xi_1(s), \xi_2(s)) \in S^3$  with  $|\xi_1(s)|^2 + |\xi_2(s)|^2 = 1$  and can be written as SU2) matrix (18). We can thus write the maximally ordered ( $\mathcal{W}_p = 1, \forall p$ ) magnetic eigenstates in (20) as the direct product of two vertex or site states defined at the two ends of the link  $l$ ,

$$|Z(\vec{l})\rangle = \sum_{j=0}^{\infty} \sum_{m=-j}^j |\xi(s)\rangle_m^j \otimes |\xi^\dagger(s')\rangle_m^j. \quad (22)$$

The site states at left and right ends ( $s$  and  $s'$ ) of the link  $\vec{l}$  are defines as

$$|\xi(s)\rangle_m^j = \sqrt{d_j} \sum_{m_+} D_{m_+, m}^j(\xi(s)) |j, m_+\rangle_l, \quad |\xi^\dagger(s')\rangle_m^j = \sqrt{d_j} \sum_{m_-} D_{m, m_-}^j(\xi^\dagger(s')) |j, m_-\rangle_l \quad (23)$$

Above  $d_j \equiv \sqrt{(2j+1)}/4\pi$ . Therefore, all states satisfying  $B_p|\psi\rangle = |\psi\rangle$  can be written as product of the site states at every site  $s$

$$|\psi\rangle = \sum_{\text{all } j} \sum_{\text{all } m} \prod_{s \in \mathcal{T}_2} |\xi(s)\rangle_{m_1}^{j_1} \otimes |\xi(s)\rangle_{m_2}^{j_2} \otimes |\xi^\dagger(s)\rangle_{m_3}^{j_3} \otimes |\xi^\dagger(s)\rangle_{m_4}^{j_4},$$

We can now perform the integrations over  $\xi(s)$  at every site  $s$  to get the loop states satisfying both the conditions in (15). Using the multiplicative properties of the Wigner rotation matrices [7], these group manifold integrations at every lattice site can be performed exactly to get

$$\begin{aligned} |\psi_0\rangle &= \sum_{\text{all } j} \sum_{\text{all } m} \prod_{s \in \mathcal{T}_2} \left\{ \int_{S^3} d^2\mu(\xi(s)) |\xi(s)\rangle_{m_1}^{j_1} \otimes |\xi(s)\rangle_{m_2}^{j_2} \otimes |\xi^\dagger(s)\rangle_{m_3}^{j_3} \otimes |\xi^\dagger(s)\rangle_{m_4}^{j_4} \right\}, \\ &= \sum_{\{\vec{J}\}} W\{\vec{J}\} \prod_s \otimes \underbrace{|j_1, j_2, j_{12} = j_{34}, j_3, j_4\rangle_s}_{\text{loop state at site } s} = \sum_{\{\vec{J}\}} W\{\vec{J}\} \prod_s \otimes |\vec{J}\rangle_s. \end{aligned} \quad (24)$$

In (24) the loop states at every site  $s$  are

$$|\vec{J}\rangle_s = \sum_{\text{all } m's} \eta(j_{12}, m_{12}) C_{j_1, m_1, j_2, m_2}^{j_{12}, m_{12}} C_{j_3, m_3, j_4, m_4}^{j_{12}, -m_{12}} |j_1, m_1\rangle_s \otimes |j_2, m_2\rangle_s \otimes |j_3, m_3\rangle_s \otimes |j_4, m_4\rangle_s. \quad (25)$$

In (25)  $\eta(j, m) \equiv (-1)^{j-m}(2j+1)^{-\frac{1}{2}}$  and the loop states  $|\vec{J}\rangle_s \equiv |j_1, j_2, j_{12} = j_{34}, j_3, j_4\rangle_s$  contain two group theoretical triangular constraints [5] around every lattice site. They are illustrated on the dual lattice plaquette in Figure 2-c. The amplitudes  $W\{\vec{J}\}$  can be computed after integrating over all  $L^2$  lattice sites and then summing over the remaining magnetic quantum numbers<sup>8</sup>. These amplitudes ensure that the triangular flux constraints are satisfied at every site. They also implement the link flux constraints (4a) over the entire torus. It is illustrative to consider a simple example and understand this construction. We consider a torus with 4 lattice sites  $A, B, C$  and  $D$  and 4 associated plaquettes as shown in Figure 3-a. The ground state in (24) can now be written as

$$|\psi_0\rangle = \sum_{\{\vec{J}_A, \vec{J}_B, \vec{J}_C, \vec{J}_D\}} \underbrace{W(\vec{J}_A, \vec{J}_B, \vec{J}_C, \vec{J}_D)}_{\text{amplitude}} \underbrace{|\vec{J}_A\rangle \otimes |\vec{J}_B\rangle \otimes |\vec{J}_C\rangle \otimes |\vec{J}_D\rangle}_{\text{loop states on torus}}. \quad (26)$$

The amplitudes  $W$  in (26) are  $12j$  Wigner coefficients of 2nd kind:

$$W(\vec{J}_A, \vec{J}_B, \vec{J}_C, \vec{J}_D) = K \begin{bmatrix} j_4^D = j_2^A & j_1^A = j_3^B & j_4^B = j_2^C & j_1^C = j_3^D & & \\ & j^A & j^B & j^C & j^D & \\ j_2^D = j_4^A & j_3^A = j_1^B & j_2^B = j_4^C & j_3^C = j_1^D & & \end{bmatrix} \quad (27)$$

We have defined  $K = \prod_{(\text{all } j)} \sqrt{(2j+1)}$ . The  $12-j$  Wigner coefficients are illustrated in Figure 3-b. The pure gauge conditions (21) make the ground state  $|\psi_0\rangle$  satisfy

$$W_{\gamma_x} |\psi_0\rangle = |\psi_0\rangle, \quad W_{\gamma_y} |\psi_0\rangle = |\psi_0\rangle. \quad (28)$$

Hence  $|\psi_0\rangle$  is in the trivial topological sector.

---

<sup>8</sup>We note that all the magnetic quantum number dependence is completely contained in the Clebsch Gordan coefficients appearing as the coefficients of the loop states

$$\begin{aligned} & \int_{S^3} d^2\mu(\xi(s)) |\xi(s)\rangle_{m_1}^{j_1} \otimes |\xi(s)\rangle_{m_2}^{j_2} \otimes |\xi^\dagger(s)\rangle_{m_3}^{j_3} \otimes |\xi^\dagger(s)\rangle_{m_4}^{j_4} \\ & = K_{\{j_1, j_2, j_3, j_4\}} (-1)^{j_3 - m_3 + j_4 - m_4} \sum_{j_{12}, m_{12}} \eta(j_{12}, m_{12}) C_{j_1, m_1, j_2, m_2}^{j_{12}, m_{12}} C_{j_3, m_3, j_4, m_4}^{j_{12}, -m_{12}} |j_1, j_2, j_{12}, j_3, j_4\rangle_s, \end{aligned}$$

where  $K_{\{j_1, j_2, j_3, j_4\}} = \prod_{\{\text{all } j\}} (2j+1)^{1/4}$ . The sums over remaining magnetic quantum numbers  $(m_1, m_2, m_3, m_4)$  can be done after integrating over all  $L^2$  lattice site on  $\mathcal{T}_2$ .



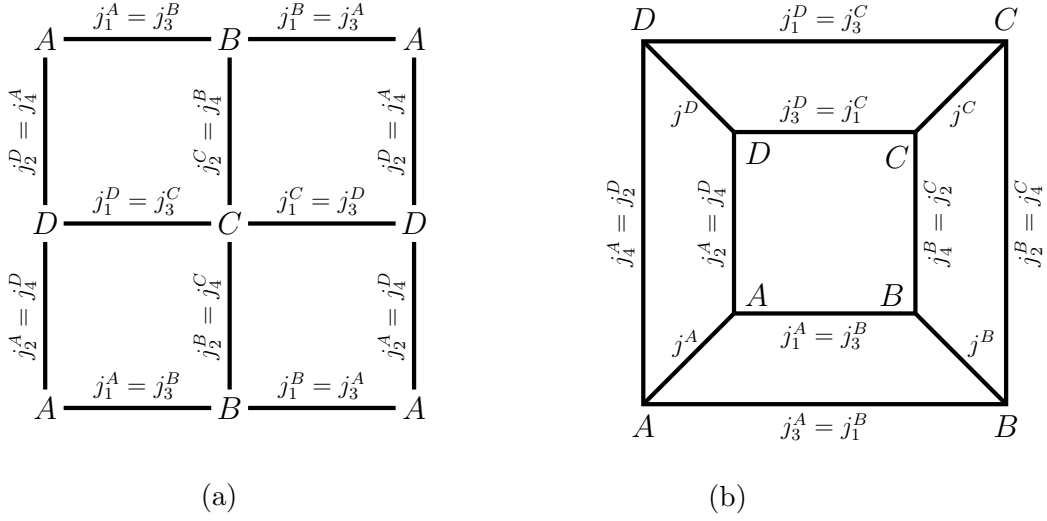


Figure 3: SU(2) toric code. (a) Electric fluxes on a 4 plaquette toric code, (b) 12-j Wigner coefficients involving 8 triangular constraints as amplitude for SU(2) toric code ground state.

### 2.1.1 $Z_N \otimes Z_N$ charges

To construct topologically nontrivial ground states carrying  $Z_N \otimes Z_N$  charges, we generalize the pure gauge conditions (21) as follows. We attach  $Z_N \otimes Z_N$  phase factors  $\eta_x$  and  $\eta_y$  to all the links along the two strips  $\mathcal{S}_y$  and  $\mathcal{S}_x$  encircling the torus as shown in Figure 4 -a,b.

$$\begin{aligned} Z(l_x) &= \xi(s) \eta(l_x) \xi^\dagger(s'), & \eta(l_x) &\equiv \eta_x = e^{\frac{2\pi i p}{N}}, & l_x &\in \mathcal{S}_y, \\ Z(l_y) &= \xi(s) \eta(l_y) \xi^\dagger(s'), & \eta(l_y) &\equiv \eta_y = e^{\frac{2\pi i q}{N}}, & l_y &\in \mathcal{S}_x. \end{aligned} \quad (29)$$

In (29),  $p, q = 0, 1, 2, \dots, (N-1)$ . Repeating the procedure of the last section after replacing (21) with (29) we get

$$|\psi_0\rangle_{(p,q)} = \sum_{\{\vec{J}\}} (\eta_x)^{\{\mathcal{J}_x\}} (\eta_y)^{\{\mathcal{J}_y\}} W\{\vec{J}\} \prod_s \otimes \underbrace{|j_1, j_2, j_{12} = j_{34}, j_3, j_4\rangle_s}_{\text{loop state at site } s}. \quad (30)$$

The additional phase factors in (30) leading to topologically non-trivial sectors are

$$\mathcal{J}_x = \sum_{l_x \in \mathcal{S}_y} j(l_x), \quad \mathcal{J}_y = \sum_{l_y \in \mathcal{S}_x} j(l_y). \quad (31)$$

The ground states  $|\psi_0\rangle_{(p,q)}$  satisfy

$$W_{\gamma_x} |\psi_0\rangle_{(p,q)} = \eta_x |\psi_0\rangle_{(p,q)}, \quad W_{\gamma_y} |\psi_0\rangle_{(p,q)} = \eta_y |\psi_0\rangle_{(p,q)}. \quad (32)$$

The ground state in the trivial sector in (24) is  $|\psi_0\rangle = |\psi\rangle_{(p=0, q=0)}$ . Having constructed all  $N^2$  ground states, we now discuss the quasiparticle excited states and then nonabelian anyons.

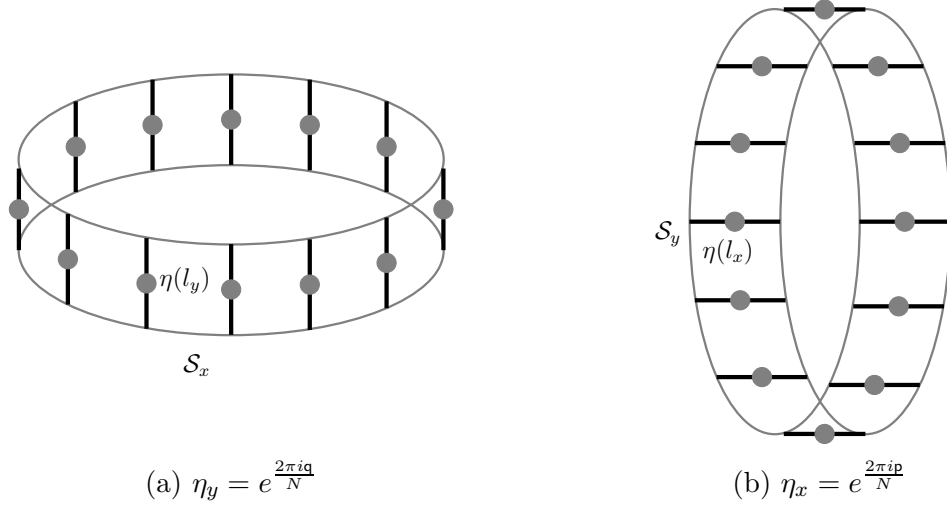


Figure 4: Construction of topologically nontrivial ground states. Inserting  $Z_N$  twist factors, shown as  $\bullet$ , in the ground states: (a)  $\eta_y$  along  $\mathcal{S}_x$ , (b)  $\eta_x$  along  $\mathcal{S}_y$ .

## 2.2 Nonabelian electric and magnetic excitations

### 2.2.1 Electric Fluxes

We now define the Wilson charge operator

$$\Gamma_{\alpha\beta}^{(N)}(n', n) = \left( \prod_{\vec{l} \in \mathcal{L}}^p U(\vec{l}) \right)_{\alpha\beta}. \quad (33)$$

In (33)  $\prod^p$  denotes the lattice path ordered product of link holonomies in the  $SU(N)$  fundamental representation along the oriented path  $\mathcal{L}$  as shown in figure 5. The string operator is invariant under rotations (6) all along  $\mathcal{L}$  except at the end point  $n$  ( $n'$ ) where it creates  $SU(N)$  quasiparticle in the fundamental  $N$  (anti-fundamental  $\bar{N}$ ) representation.

$$\begin{aligned} [A_m, \Gamma_{\alpha\beta}^{(N)}(n', n)] &= \frac{(N^2 - 1)}{N^2} \Gamma_{\alpha\beta}^{(j)}(n', n), & \text{if } m = n \text{ or } n', \\ &= 0 & \text{otherwise.} \end{aligned} \quad (34)$$

We also note that the length and shape of the string  $\mathcal{L}$  between the end points are invisible and therefore unphysical. As  $U_{\alpha\beta}(l)$  commute amongst themselves,

$$[B_p, \Gamma_{\alpha\beta}^{(N)}(n', n)] = 0. \quad \forall p; n', n. \quad (35)$$

Thus the quasiparticle states

$$|\psi_{\alpha\beta}^{(N)}(n', n)\rangle_{(p,q)} \equiv \Gamma_{\alpha\beta}^{(N)}(n', n) |\psi_0\rangle_{(p,q)} \quad (36)$$

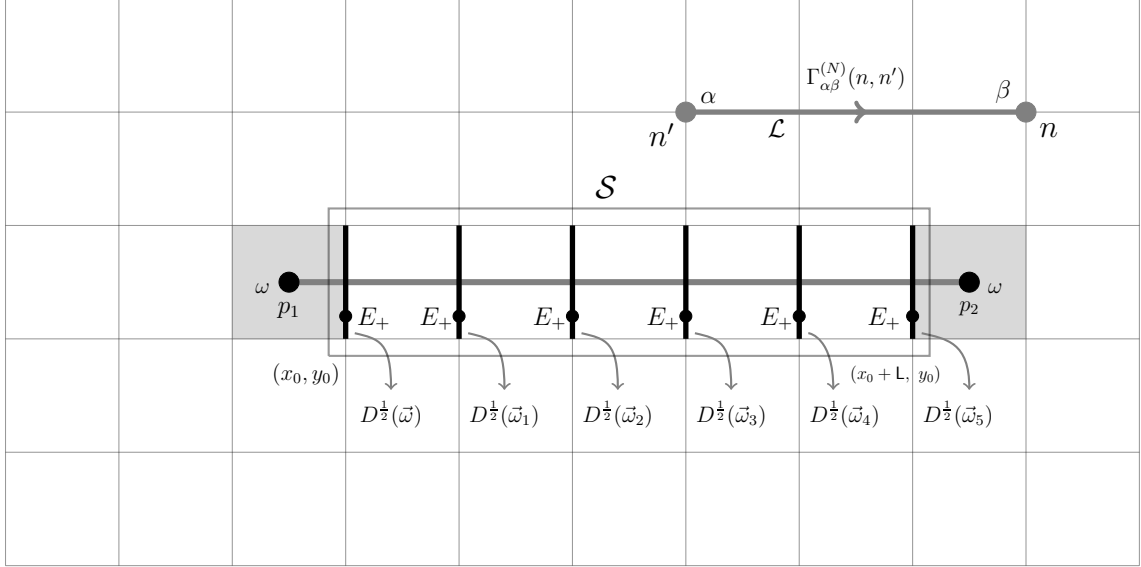


Figure 5: Creating electric charges at sites and magnetic vortices on plaquettes. The operator  $\Gamma_{\alpha\beta}^{(N)}(n', n)$  creates electric charges in the fundamental representations at the two end points  $n$  and  $n'$ . The operator  $\Sigma_{\vec{\omega}}$  acts on all the vertical link fluxes  $U(n; \hat{2}) \in \mathcal{S}$  and rotates all of them by  $\omega$ . The rotation axes  $\hat{\omega}_1, \hat{\omega}_2, \dots, \hat{\omega}_L$  are related to  $\hat{\omega}(x_0, y_0)$  by parallel transports (40). Note that the shapes and lengths of  $\mathcal{L}$  and  $\mathcal{S}$  are invisible.

are the eigenstates of the  $SU(N)$  toric code Hamiltonian (9)

$$H |\psi_{\alpha\beta}^{(N)}(n', n)\rangle_{(p,q)} = 2A \frac{(N^2 - 1)}{N^2} |\psi_{\alpha\beta}^{(N)}(n', n)\rangle_{(p,q)}. \quad (37)$$

Therefore,  $|\psi_{\alpha\beta}^{(N)}(n', n)\rangle_{(p,q)}$  are the eigenstates of  $H$  with quasiparticles in the fundamental (anti-fundamental) representations at lattice sites  $n$  ( $n'$ ). We can similarly construct electric states in the higher representations of  $SU(N)$ . These state will be characterized by the corresponding  $SU(N)$  Young tableau.

## 2.2.2 Magnetic fluxes

We now construct unitary vortex operators which create and destroy nonabelian magnetic fluxes on two plaquettes [6]. The  $SU(2)$  magnetic fluxes on the plaquettes in the axis, angle  $\vec{\omega} \equiv (\hat{\omega}, \omega)$  representation can be written as

$$\mathcal{W} = \cos\left(\frac{\omega}{2}\right) \sigma_0 + i \hat{\omega} \cdot \vec{\sigma} \sin\left(\frac{\omega}{2}\right). \quad (38)$$

To construct vortex or disorder operator creating the above magnetic flux we consider a finite length ladder strip<sup>9</sup>  $\mathcal{S}$  which extends from the plaquette  $p_1$  to the plaquette  $p_2$  as shown in Figure 5. We now write the SU(2) vortex pair creation operator as

$$\Sigma_{\vec{\omega}}(p_2, p_1) = \exp i \left( \sum_{i=0}^L \hat{\omega}(x_0 + i, y_0) \cdot \vec{E}_+(x_0 + i, y_0, \hat{2}) \right) \frac{\omega}{2}. \quad (39)$$

The axes of rotations along the ladder strip  $\mathcal{S}$  are related to  $\hat{\omega} \equiv \hat{\omega}(x_0, y_0)$  by parallel transports:

$$\hat{\omega}^a(x_0 + i, y_0) = R_b^a(S(x_0, y_0 \rightarrow x_0 + i, y_0)) \hat{\omega}^b(x_0, y_0) = R_b^a(S(x_0, y_0 \rightarrow x_0 + i, y_0)) \hat{\omega}^b. \quad (40)$$

The parallel transport in (40) along the flux string  $S$  is chosen to be along a straight horizontal line for convenience:  $S(x_0, y_0 \rightarrow x_0 + i, y_0) \equiv U(x_0, y_0; \hat{1}) U(x_0 + 1, y_0; \hat{1}) \cdots U(x_0 + i - 1, y_0, \hat{1})$  and  $R_b^a(S) = \frac{1}{2} \text{Tr}(\sigma^a S \sigma^b S^\dagger)$ . The vortex operator  $\Sigma_{\vec{\omega}}(p_2, p_1)$  creates magnetic vortices on the plaquettes  $p_1$  and  $p_2$  located at the end points of the ladder strip  $\mathcal{S}$ . All other plaquette magnetic fluxes along  $\mathcal{S}$  remain zero. Therefore, we define a magnetic vortex state

$$|\psi_{\vec{\omega}}(p_2, p_1)\rangle_{(\mathbf{p}, \mathbf{q})} \equiv \Sigma_{\vec{\omega}}(p_2, p_1) |\psi_0\rangle_{(\mathbf{p}, \mathbf{q})}. \quad (41)$$

These are states with magnetic vortices on the plaquettes  $p_1$  and  $p_2$

$$\begin{aligned} B_p |\psi_{\vec{\omega}}(p_2, p_1)\rangle_{(\mathbf{p}, \mathbf{q})} &= 2 \cos\left(\frac{\omega}{2}\right) |\psi_{\vec{\omega}}(p_2, p_1)\rangle_{(\mathbf{p}, \mathbf{q})}, & \text{if } p = p_1 \text{ or } p_2 \\ &= |\psi_{\vec{\omega}}(p_2, p_1)\rangle_{(\mathbf{p}, \mathbf{q})} & \text{otherwise.} \end{aligned} \quad (42)$$

The vortex operator  $\Sigma_{\vec{\omega}}(p_2, p_1)$  is invariant under (6)

$$A_n |\psi_{\vec{\omega}}(p_2, p_1)\rangle_{(\mathbf{p}, \mathbf{q})} = 0, \quad \forall n, p_1, p_2. \quad (43)$$

Therefore, they are the eigenstates of the toric code Hamiltonian (9)

$$H |\psi_{\vec{\omega}}(p_2, p_1)\rangle_{(\mathbf{p}, \mathbf{q})} = 4B \left(1 - \cos\left(\frac{\omega}{2}\right)\right) |\psi_{\vec{\omega}}(p_2, p_1)\rangle_{(\mathbf{p}, \mathbf{q})}. \quad (44)$$

We note that unlike electric charge sector, the magnetic vortex spectrum is continuous. However, we a gap can be created in the magnetic sector also by putting an extra term in (9) which relates  $A_n$  with  $B_p$ .

### 3 Nonabelian Anyons

After having discussed the  $N^2$  degenerate ground states and their electric, magnetic excitations, we now briefly analyze their nonabelian anyonic nature. As we will see, the nonabelian nature

---

<sup>9</sup>Like the the invisible string  $\mathcal{L}$  associated with the Wilson charge operators (33), the path  $\mathcal{S}$  is also invisible. Only the location of the end plaquettes  $p_1, p_2$  matters.

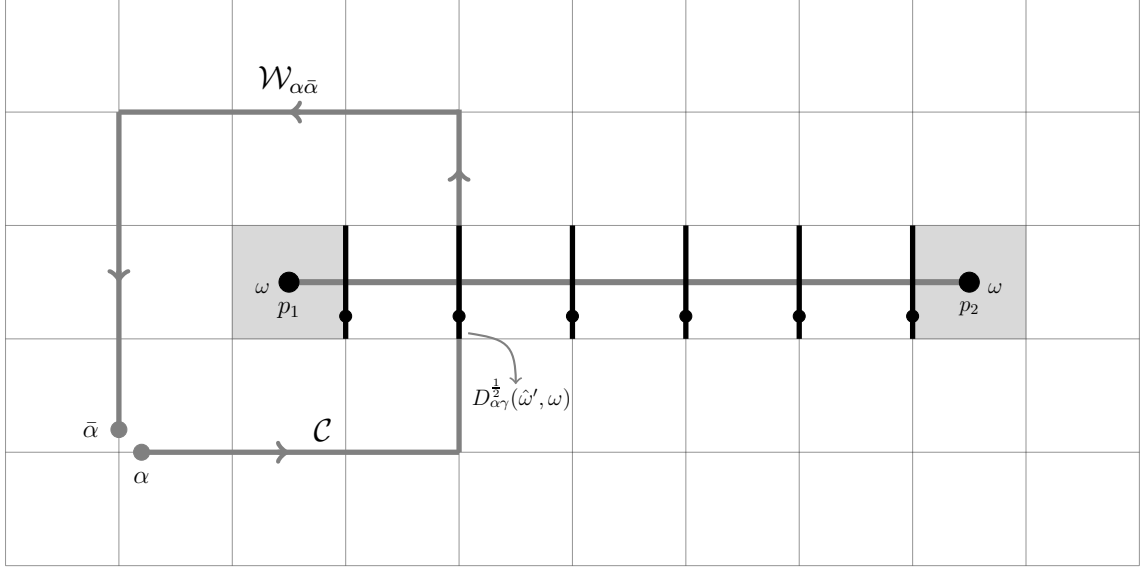


Figure 6: Taking a charge around close loop  $\mathcal{C}$  produces a nonabelian rotation by Wigner rotation matrix if a vortex is enclosed as shown in (47).

originates from the basic nonabelian canonical commutation relations (1). This is also the case with the Kitaev's toric code model. We consider taking a charged particle in the fundamental representation around a loop  $\mathcal{C}$ . This is shown in Figure 6. Using the canonical commutation relations between the electric fields and the potentials (1) we get

$$\begin{aligned}
 \Sigma_{\vec{\omega}}(p_2, p_1) \mathcal{W}_{\alpha\beta}(\mathcal{C}) \Sigma_{\vec{\omega}}^{-1}(p_2, p_1) &= D_{\alpha\gamma}^{j=\frac{1}{2}}(\hat{\omega}', \omega) \mathcal{W}_{\gamma\beta}(\mathcal{C}), & \text{if } \mathcal{C} \text{ encloses } p_1, \\
 &= D_{\alpha\gamma}^{j=\frac{1}{2}}(\hat{\omega}'', \omega) \mathcal{W}_{\gamma\beta}(\mathcal{C}), & \text{if } \mathcal{C} \text{ encloses } p_2, \\
 &= \mathcal{W}_{\alpha\beta}(\mathcal{C}). & \text{otherwise.}
 \end{aligned} \tag{45}$$

Thus an electric charge encircling a vortex undergoes SU(2) rotation by Wigner matrix<sup>10</sup>. This can be seen as follows. We consider the following initial and final states:

$$|I\rangle_{\alpha\beta}^{(\omega)} \equiv \Sigma_{\vec{\omega}} \Gamma_{\alpha\beta}^{(j=1/2)}(n, n') |\psi_0\rangle_{\mathbf{p}, \mathbf{q}}, \quad |F\rangle_{\alpha\beta}^{(\omega)} \equiv \mathcal{W}_{\alpha\bar{\alpha}}(\mathcal{C}) \Sigma_{\vec{\omega}} \Gamma_{\bar{\alpha}\beta}^{(j=1/2)}(n, n') |\psi_0\rangle_{\mathbf{p}, \mathbf{q}}. \tag{46}$$

Both the initial and the final states are in the  $(\mathbf{p}, \mathbf{q})$  sector. Using (45) we get

$$\begin{aligned}
 |F\rangle_{\alpha\beta}^{(\omega)} &= D_{\alpha\bar{\alpha}}^{j=\frac{1}{2}}(\hat{\omega}', \omega) |I\rangle_{\bar{\alpha}\beta}^{(\omega)}, & \text{if } \mathcal{C} \text{ encloses a vortex,} \\
 &= |I\rangle_{\alpha\beta}^{(\omega)}, & \text{otherwise.}
 \end{aligned} \tag{47}$$

<sup>10</sup>In (45) the unit vector  $\hat{\omega}'$  and  $\hat{\omega}''$  are related to unit vector  $\hat{\omega}$  through parallel transports which depend on the shapes, sizes of the string  $\mathcal{S}$  as well as  $\mathcal{C}$ . Therefore, axes orientations are unphysical. However, the magnitude  $\omega$  is invariant under (6) and is also robust against any deformations or choices of the closed curve  $\mathcal{C}$  or  $\mathcal{S}$  in Figure 6.

The above result is illustrated in Figure 6. We note that the topological indices  $(\mathbf{p}, \mathbf{q})$  are not detected by the Wilson loop  $\mathcal{W}(\mathcal{C})$  in (47). This is an expected result as no local measurement can distinguish different topological sectors. We can also consider the electric charges in the higher  $j$  representations leading to the Wigner rotation matrices  $D_{mm'}^j(\hat{\omega}', \omega)$  as the matrix on the right hand side of (45). We note that the composites of  $\Gamma$  and  $\Sigma$  have both electric and magnetic charges and behave like dyons. Their mutual interchange or braiding will lead to nonabelian anyonic statistics.

## 4 Summary and discussion

In this work we have constructed and analyzed SU(N) toric code model. The  $N^2$  topologically stable ground states and all possible electric, magnetic excitations are obtained. The electric charge and magnetic vortex creation-annihilation operators and their relative nonabelian anyonic nature is discussed. We expect that these nonabelian models will also have potential applications in topological quantum computing in the future. In the recent past, there has been immense activities to simulate non-abelian lattice gauge theory Hamiltonians using cold atomic gases and optical lattices [8]. We hope such attempts will also lead to physical realization of nonabelian toric code Hamiltonians and their topologically stable Hilbert spaces consisting of robust group theoretical spin networks.

**Acknowledgements:** We would like to thank Diptiman Sen for useful discussions.

## References

- [1] A. Yu. Kitaev, Fault-tolerant quantum computation by anyons, *Annals of Phys.*303, 2-30 (2003), arXiv: quant-ph/9707021.
- [2] C. Nayak, S. H. Simon, M. Freedman and S. D. Sarma, Non-Abelian anyons and topological quantum computation, *Rev. Mod. Phys.*801083 (2008), Bernard Field and Tapio Simula, 2018 *Quantum Sci. Technol.* 3 045004, arXiv:1802.06176 [quant-ph].
- [3] Preskill, Lecture notes for Physics 219: Quantum computation <http://www.theory.caltech.edu/~preskill/ph219/topological.pdf>; Sumathi Rao, Introduction to abelian and non-abelian anyons, *Topology and Condensed Matter Physics. Texts and Readings in Physical Sciences*, vol 19. Springer, Singapore.
- [4] Kogut and L. Susskind, *Phys. Rev. D*11, 395 (1975).
- [5] D. Robson and D. M. Webber, *Z. Phys.* C15, 199 (1982); W. Furmanski and A. Kolawa, *Nucl. Phys.*B291, 594(1987); R. Anishetty and H. S. Sharatchandra, *Phys. Rev. Lett.*65, 813 (1990); G. Burgio, R. De Pietri, H. A. Morales-Tecotl, L. F. Urrutia and J. D. Vergara,

- Nucl. Phys.B566, 547 (2000); Manu Mathur, Nucl. Phys. B 779, 32 (2007), [arXiv:hep-lat/0702007].
- [6] Manu Mathur and T. P. Sreeraj, Phys. Rev. D94, 085029 (2016); Manu Mathur and T. P. Sreeraj, Phys. Rev. D92, 125018(2015).
- [7] D. A. Varshalovich, A. N. Moskalev and V. K. Khersonskii, Quantum Theory of Angular Momentum, World Scientific 1988.
- [8] M.C. Banuls et al., Simulating Lattice Gauge Theories within Quantum Technologies, arXiv:1911.00003v1 ; E. Zohar and B. Reznik, Phys. Rev. Lett. 107, 275301 (2011); E. Zohar, J. I. Cirac, and B. Reznik, Phys. Rev. Lett. 109, 125302 (2012), Lukas Homeier, Christian Schweizer, Monika Aidelsburger, Arkady Fedorov, Fabian Grusdt, Phys. Rev. B 104, 085138 (2021); Yu Tong, Victor V. Albert, Jarrod R. McClean, John Preskill, Yuan Su, arXiv:2110.06942; Zohreh Davoudi, Mohammad Hafezi, Christopher Monroe, Guido Pagano, Alireza Seif, and Andrew Shaw Phys. Rev. Research 2, 023015.